



Effect of nitrogen-plasma surface treatment to the enhancement of TiO₂ photocatalytic activity under visible light irradiation

Chao-Ming Huang^{a,*}, Lung-Chuan Chen^b, Kong-Wei Cheng^c, Guan-Ting Pan^a

^a Department of Environmental Engineering, Kun Shan University, Yung Kang City, Tainan 710, Taiwan, ROC

^b Department of Polymer Materials, Kun Shan University, Yung Kang City, Tainan 710, Taiwan, ROC

^c Energy and Environment Laboratory, Industrial Technology Research Institute, Hsin Chu 310, Taiwan, ROC

Received 12 June 2006; received in revised form 1 August 2006; accepted 2 August 2006

Abstract

A visible-light-active commercial TiO₂ powder was prepared by thermal nitrogen-plasma processing as the surface treatment. The photoactivity of the treated TiO₂ samples was evaluated in the photocatalytic degradation of gaseous 2-Propanol (IPA) in a batch reactor. XPS analysis showed that oxygen vacancies formed in the lattice of the treated TiO₂ particles and no nitrogen peaks were detected. With increasing the treating time, the visible absorbance and oxygen vacancies were increased but the surface area of treated sample was decreased. The photodegradation rate of IPA under visible light illumination depended strongly on the treating time of the catalyst, and the photoactivity of the treated sample was higher than that of plain TiO₂. From the results of reaction rate constant and mineralization yield of IPA, it was found that the TiO₂ powders treated for 30 min demonstrated the highest photocatalytic activity among all samples. This high visible light photoactivity was ascribed to an intermediate level of visible absorbance as well as optimal oxygen vacancies after the thermal nitrogen-plasma surface treatment.

© 2006 Elsevier B.V. All rights reserved.

Keywords: TiO₂; Thermal nitrogen-plasma processing; Oxygen vacancies; Mineralization yield

1. Introduction

TiO₂ is widely used for the mineralization of environmental pollutants including organic or inorganic and it exhibits strong oxidation activity under ultraviolet light with a wavelength of 390 nm or less. Since ultraviolet (UV) light is only 3–5% part of the solar spectrum, the photocatalytic activity of TiO₂ is not enough under the visible and/or solar light irradiation. It would be very valuable to develop visible-light-active TiO₂ photocatalysts that can yield efficient reaction under solar light for industrial areas or poor interior lighting illumination in living spaces. In the last decade, the studies of doping TiO₂ with different transition metal ions [1,2] to reduce the band gap were intensively investigated, but their efficiency would be reduced due to the formation of electron-hole recombination center. There have recently been a number of reports on non-metal doped-TiO₂ with anions of N [3], C [4], and S [5], which caused photo-responses in the visible-light region. Although the visible-light-active pho-

tocatalysis of N-doped TiO₂ has been confirmed by many studies, the mechanism of nitrogen that contributes the enhancement of photocatalytic activity remains unclear. For example, Asahi et al. [6] prepared nitrogen doped TiO₂ films by sputtering TiO₂ in a N₂/Ar gas mixture, and then post-annealing at 550 °C in N₂ gas for 4 h. From the XPS analysis, they acclaimed three N 1s peaks with binding energies of 402, 400, and 396 eV were observed and concluded that the 396 eV is indispensable for visible-light activity of N-doped TiO₂. A similar N-doping of TiO₂ film was reported by Yang et al. [7]. They made the TiO_{2-x}N_x films by ion-assisted electron-beam evaporation and also found N 1s peaks at 402 and 396 eV. On the other hand, the chemical state for doped N, Sato et al. [8] prepared N-doped TiO₂ powders by sol-gel method using titanium tetra-isopropoxide or TiCl₄ with aqueous ammonia solution and found only the peak at 400 eV was certainly detected but exhibit no peak at 396 eV. Li et al. [9] studied the N-doped process of TiO₂ powders by spray pyrolysis from TiCl₄ and different N-precursors; however, the XPS analysis indicated no nitrogen peaks were detected in their samples. In addition, Ihara et al. [10] prepared visible-light active TiO₂ powders by the hydrolysis of Ti(SO₄)₂ with an aqueous ammonia solution and ruled out N-doping to be effective for

* Corresponding author. Tel.: +886 6 2050359; fax: +886 6 2050540.
E-mail address: charming@mail.ksu.edu.tw (C.-M. Huang).

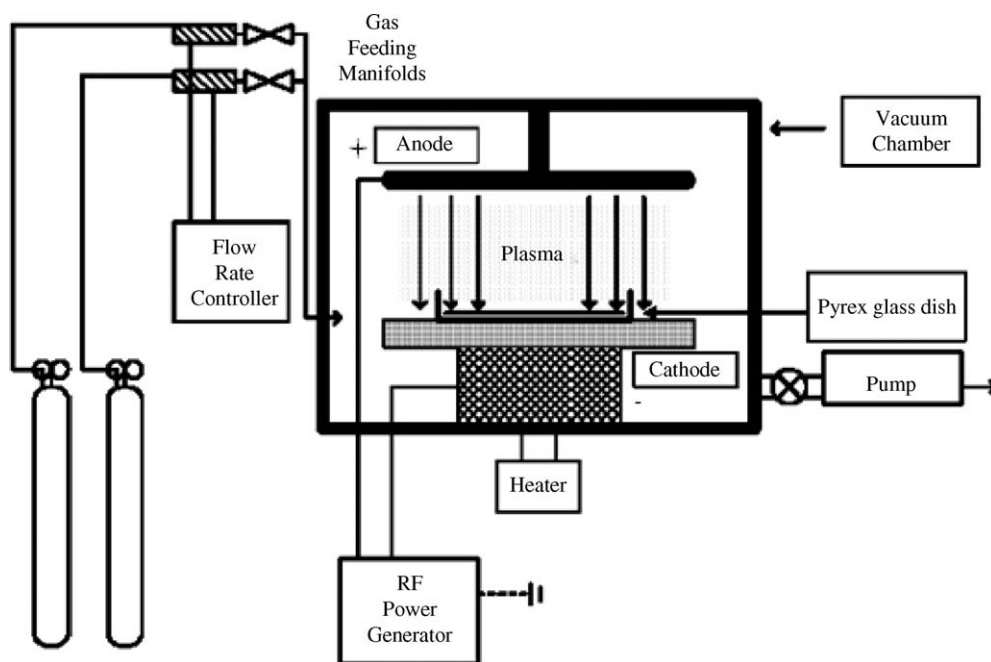


Fig. 1. Scheme of apparatus for plasma surface-treatment over TiO₂ powders.

visible-light activity, since N was a trace amount (0.2%). They concluded that the function of N dopant in TiO₂ was to retard the reoxidation of oxygen-deficient sites which cause visible-light activity. They also confirmed the role of oxygen vacancies in the TiO₂ powders treated with low-temperature H₂ plasma, which is essentially indispensable for visible light sensitization. In view of these results, it is quite obvious that without the bombardment of high-energy nitrogen species, no or very little nitrogen atoms can be incorporated in the TiO₂. Up to date, the contribution of doped nitrogen atoms or oxygen vacancies to the visible-light activity of TiO₂ remains unclear. The relation between the role of oxygen vacancies and the corresponding visible-light-active photocatalytic property has not yet been well investigated. Hence, the purpose of this study is to investigate the variations of photocatalytic properties induced by oxygen vacancies due to the thermal nitrogen-plasma surface treatment. The photocatalytic activities of plain and the plasma-heat treated TiO₂ powders were characterized by 2-Propanol photodegradation under the interior daylight lamp.

2. Experimental

2.1. Materials

The anatase TiO₂ powder (ST-01, Ishihara Sangyo) was chosen as the raw material with the average crystallite size of 6.87 nm determined by X-ray diffraction (XRD). The analytical grade of 2-Propanol was procured from Merck (Germany).

2.2. Preparation of plasma surface-treatment of TiO₂

The surface modification of ST-01 samples were prepared in a stainless steel chamber (12.84 L) with 13.56 MHz radio

frequency (RF) power supply (Dressler Hochfrequenztechnik, VM700A) and an automatic impedance matching unit (AMN-100), shown in Fig. 1. The ST-01 powders of 0.5 g were spread out evenly in a Pyrex glass dish and then introduced on the cathode electrode. The chamber was started to vacuum and heating. The temperature of cathode electrode was controlled and monitored with a thermocouple positioned at the backside of the cathode electrode separated from the anode electrode by 3.5 cm. When the chamber was evacuated to a background pressure of 10⁻⁵ Pa, pure gas of N₂ (99.9995%) was introduced to the chamber. After the pressure and temperature reached to the predetermined values, the plasma was started. Throughout this work, the flow rate of N₂ was kept at constant value of 10 sccm, RF power of 400 W and working pressure at 30 Pa. Conditions for the thermal plasma treatment of powders were investigated by changing treatment period (10–120 min) at 400 °C.

2.3. Analyses of photocatalysts

The crystallinity of TiO₂ samples was verified by XRD (Rigaku DIMAX-2500V/PC, Cu K α radiation) and their diffraction patterns were measured at an angle of 2 θ from 5 to 60°. BET surface area measurements of TiO₂ before and after plasma-heat modifications were carried out by N₂ adsorption at 77 K (Micromeritics ASAP 2020). The surface composition and chemical state of the TiO₂ were examined by X-ray photoelectron spectroscopy (XPS, Omicron Multiprobe Compact) using a monochromatic Al K α source and the binding energy scale was calibrated to 284.6 eV for C 1s peak. The UV–vis absorbance spectra of raw and treated ST-01 samples were measured by a Hitachi U-3010 spectrophotometer, equipped with an integrating sphere, and a Ba₂SO₄ standard white plate as reference.

2.4. Photocatalytic experiments

0.1 g of TiO₂ powder was uniformly spread over the center of a horizontal Pyrex glass reactor of 1520 cm³ capacity (48 cm height, 8.4 cm i.d.) and was illuminated by a white fluorescent light lamp (TFC, FL10W-EX) or an ultraviolet lamp (PHILIPS, TLD 10 W/08). The light intensity on the surface of powder was 0.2 mW/cm² for visible light and 1.61 mW/cm² for ultraviolet light, respectively. The adsorption and photocatalytic decomposition of gas-phase IPA onto TiO₂ powders were evaluated at room temperature (22 ± 2 °C). Then, liquid IPA was injected into the reactor. Right after vaporization, the IPA samples were withdrawn from a sampling port on the side of the reactor using a microsyringe and injected into the gas chromatograph (Perkin-Elmer, Clarus 500) equipped with a 60 m × 0.53 mm DB-624 capillary column and a thermal conductivity detector to measure the IPA and CO₂ concentrations. The final product of photocatalytic reaction, CO₂, was calibrated using standard CO₂ gas from Supelco Co.

3. Results and discussion

3.1. Characterization comparison of plain and plasma-treated TiO₂

The color of thermal plasma-treated sample was changed from beige to light grey by visible observation depending on the treatment time. The more plasma-heat treatment TiO₂ sample is, the more colored it is. The absorption spectra of TiO₂ samples were shown in Fig. 2. Compared with plain TiO₂, the plasma-heat samples exhibited an obvious absorbance in the visible light region during 400–600 nm. This absorbance increase shifts gradually to higher value as the treating time of powder increases, which implies that thermal RF plasma is an effective technique for the increase of visible light absorption of TiO₂ powders. Several studies [7,9,11] based on nitrogen-doped TiO₂ photocatalysts have been reported that the visible absorption intensity and shift of the absorption shoulder are increased with increasing N-doped concentration. In this study, the shift of the absorption edge of treated TiO₂ was not observed in the visible light region. The XRD diffraction patterns of ST01 before and

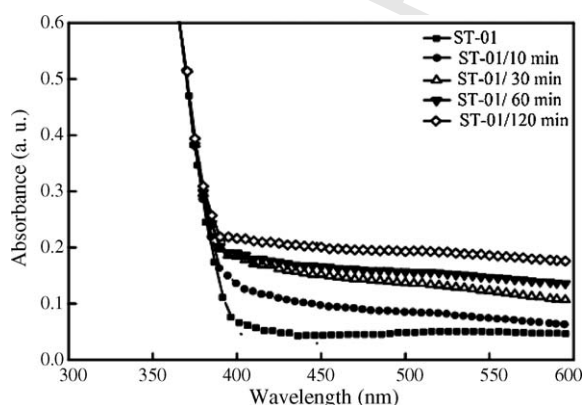


Fig. 2. Optical absorbance spectra of TiO₂ powders before and after N₂-plasma treatment for different treatment time at 400 °C.

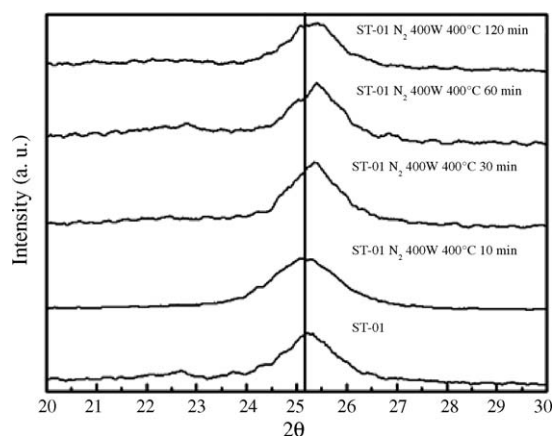


Fig. 3. XRD diffraction patterns of plain and N₂-plasma heat-treated TiO₂ powders.

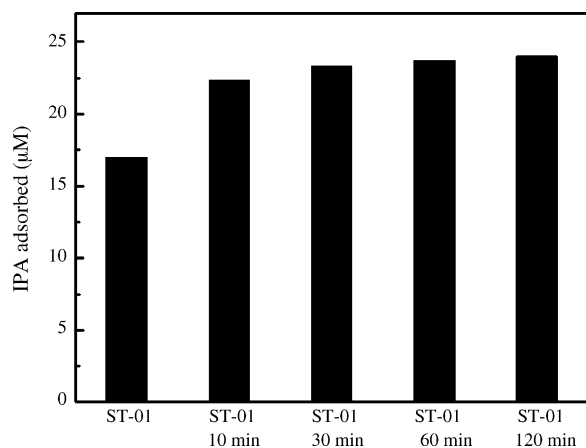
after plasma-heat treatment indicated that thermal N₂-plasma treatment did not result in any significant phase transfer of ST01. However, the position of the principal (1 0 1) peak shifts gradually to higher diffraction angle with increasing plasma treating time, as shown in Fig. 3. This result implies that oxygen ions are substituted by nitrogen ions, due to the smaller radius of nitrogen ions compared to oxygen ions. The results for surface area measurement and pore structure of TiO₂ powders are shown in Table 1. It can be seen that with increase of treating time leads to the decrease of surface area and the increase of pore diameter, which is attributed to the growth of TiO₂ crystallites due to sintering effect. The founding was different with that of Ihara et al. [12]. They prepared thermal hydrogen plasma treatment of TiO₂ (ST-01) and found that there was no significant change of surface area between the raw and treated ST-01 at 400 °C for 60 min.

3.2. Photoactivity of plain TiO₂ and plasma-treated TiO₂

The photocatalytic decomposition of gaseous IPA was carried out at initial concentration of 25.0 μM. After the adsorption equilibrium of the IPA onto TiO₂ was established (approximately 120 min), the visible light illumination was started. The adsorbed gaseous IPA on a 0.10 g sample at 25 °C was calculated from the difference between the initial and equilibrium concentrations. Fig. 4 shows the adsorption behavior of the IPA over various TiO₂ powders at different treatment conditions. The amount of IPA adsorbed on thermal plasma-treated sample was higher than that of ST-01 and increased with prolonging treating time. The photodegradation of IPA by TiO₂ particles

Table 1
Effect of treating time on surface characterizations of TiO₂ powders

Sample	Surface area (m ² /g)	Pore volume (nm)	Pore size (nm)
ST-01	323.39	0.59	7.64
ST-01/10 min	313.70	0.58	7.55
ST-01/30 min	294.83	0.57	7.70
ST-01/60 min	276.07	0.55	7.77
ST-01/120 min	261.08	0.56	7.98

Fig. 4. IPA adsorbed on plain and N₂-plasma heat-treated TiO₂ powders.

before and after N₂ plasma-heat treatment at 400 °C was shown in Fig. 5. After 100 min of irradiation, the photodecomposition of IPA proceeded to completion when 30 and 60 min plasma-heat treated TiO₂ particles are used, while only 40% of IPA gas has been oxidized using plain TiO₂ during the same time. Also, a longer irradiation time was required for TiO₂ treated over 10 or 120 min. It has been reported that the photocatalytic degradation systems generally follow a Langmuir–Hinshelwood (L–H) kinetic model [13–16], which can be simplified to a pseudo-first-order expression and apparent rate constant can be determined by linear regression of the data $\ln(C_0/C)$ versus the exposure time (t), where C_0 is the initial reaction concentration of the reactant and C is the concentration of the reactant at time t . So, photocatalytic activity of various TiO₂ particles was evaluated by comparing the apparent rate constants. The apparent rate constant of TiO₂ sample under visible irradiation was indicated in Table 2. According the values of apparent rate constant, the following comparisons can be drawn: (1) the photocatalytic activity of TiO₂ powders greatly depends on thermal plasma condition; the maximum activity was observed for TiO₂ powder treated for 30 min, and it was much higher than that of plain TiO₂ and (2) high visible absorption and IPA adsorption could not significantly improve the visible photoactivity, especially for TiO₂

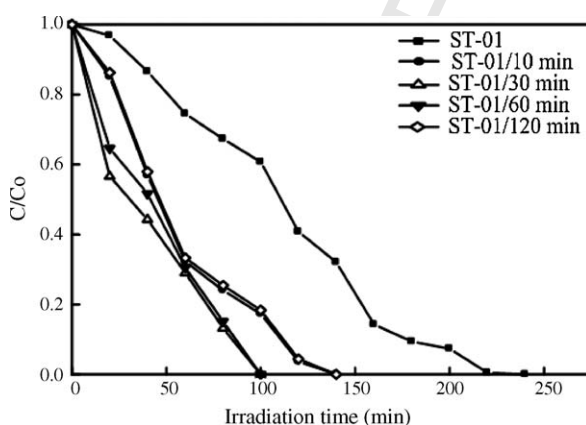
Fig. 5. Photodegradation of IPA (25.00 µM) over plain and N₂-plasma heat-treated TiO₂ powders under visible light irradiation.

Table 2

Effect of treating time on apparent rate constant of TiO₂ powders under visible light irradiation

Sample	Apparent rate constant (h ⁻¹)
ST-01	0.32
ST-01/10 min	1.10
ST-01/30 min	1.27
ST-01/60 min	1.21
ST-01/120 min	1.09

powder treated for 120 min. It can also be noticed that for this sample (400 °C for 120 min) possesses the lowest surface area (Table 1), but it has the most active surface for the highest light absorption and reactant adsorption, which is probably caused by the formation of new active sites on this treated TiO₂ powder. Similar result was reported by Ihara et al. [10]. They found the TiO₂ containing SO₄²⁻ had specific lowest surface and highest adsorption amount of acetone, but showed no vis-activity under blue-light-emitting diodes illumination. Besides, Li et al. [9] claimed that the visible absorption was directly related to the amount of N-concentration over TiO₂ particles, but only N-doping could not exhibit efficient visible photoactivity. However, the maximum photocatalytic activity was observed for N-F-codoping TiO₂, where F-doping led to the formation of surface acid sites resulting in high adsorptivity and enhanced photoactivity. To identify the chemical states of the TiO₂ powders, XPS analyses were conducted. The XPS results of the TiO₂ samples before and after treatment are shown in Fig. 6. In all samples, the

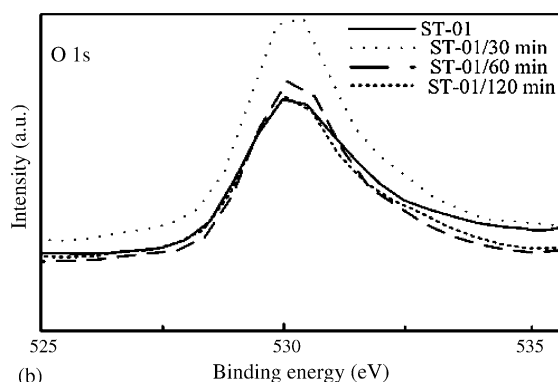
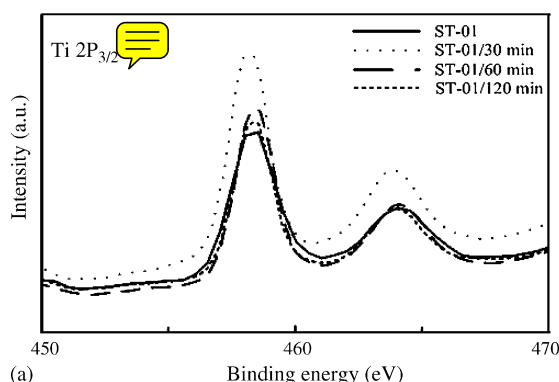
Fig. 6. XPS spectrum of (a) Ti 2p_{3/2} and (b) O 1s levels for plain and N₂-plasma heat-treated TiO₂ powders.

Table 3
Effect of treating time on the O/Ti ratio of TiO₂ powders

Sample	ST-01	ST-01/10 min	ST-01/30 min	ST-01/60 min	ST-01/120 min
O/Ti ratio	2	1.96	1.86	1.84	1.72

binding energies of Ti (2p_{3/2}) and Ti (2p_{1/2}) are present at 458.5 and 464.2 eV, respectively. The separation between Ti (2p_{3/2}) and Ti (2p_{1/2}) signals is 5.7 eV, which is consistent with characteristic XPS signals for TiO₂ [17]. However, XPS measurements of the treated samples did not show any evidence of the presence of N 1s peaks at 396 or 400 eV in this work. Although the increase in visible-light absorption of TiO₂ by N-doping has been confirmed by many studies, the N-doping for improving the visible-light activity is still unclear. Several researchers [8,18,19] acclaimed that N 1s peak at 396 eV was difficult to detect, which is quite different with the reports by Asahi et al. [6] and Yang et al. [7]. On the other hand, Ihara et al. [10] found that the trace amount of N (0.2%) was effective to suppress the reoxidation of the oxygen vacancies of TiO₂, which is responsible for visible-light photocatalytic activity. Also, they found out that the new formation of oxygen vacancy state, the sub-band gap level between the valence and the conduction bands of TiO₂, was essentially indispensable for the visible light activity of H₂-plasma-treated TiO₂ [12,20,21]. In order to find the presence and alteration of oxygen vacancies of TiO₂ samples in our study, the O:Ti atomic ratios based on XPS spectrum were indicated in Table 3. When treated with thermal N₂-plasma, the value of O/Ti ratio decreased as the treating time increased, indicating that the oxygen vacancies are produced in the lattice of the plasma-heat ST-01 particles. It is worth to discuss the interaction between N₂ and TiO₂ during the thermal N₂-plasma treatment. For the treating time, the interaction could be divided into three stages: owing to not enough energy, the relatively weak interaction between nitrogen molecules and TiO₂ resulted in a little change of O/Ti ratio at the sample treated for 10 min; as the treating time was increased to 30 and 60 min, the heating energy was enough to excite the TiO₂ and nitrogen atoms interacted effectively with the O atoms in the lattice of TiO₂, which cause the formation of oxygen vacancies; In the case of 120 min, more energy was supplied and the interaction between nitrogen molecules and TiO₂ was drastic, which led to the obvious increase of the oxygen vacancies. Compared the experimental results with oxygen vacancies, it can be seen that further increase of oxygen vacancies leads to the increase of visible absorption, but photoactivity of treated TiO₂ decreases as the oxygen vacancies increased. For the visible absorption, it might be due to the Ti³⁺ effect stated by Ishigaki et al. [22]. They pointed out that the formation of Ti³⁺ was related to color change of TiO₂, while the color was white or beige if the concentration of Ti³⁺ was low. In our study, the unique non-equilibrium situation of plasma and the time-dependent of heating are able to make the electrons already in the oxygen vacancies be driven and transferred to Ti⁴⁺, which results in the generation of Ti³⁺. Therefore, the more oxygen vacancies were produced as a result of the greater introduction of Ti³⁺ in its structure when the treating time was increased.

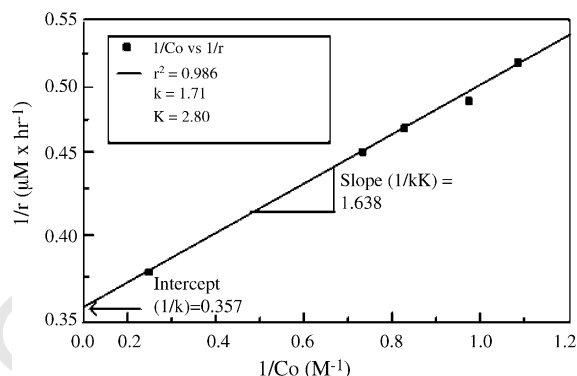


Fig. 7. Linearized plot of $1/r_{\text{IPA}}$ against $1/C_{\text{IPA}}$ for N₂-plasma heat (400 °C for 30 min) treated TiO₂.

This explained why the visible absorption was higher as oxygen vacancies increased.

Since the oxygen vacancies of TiO₂ samples treated for 30 and 60 min were very close, these two samples were chosen to further investigate the effect of treating time on the photocatalytic degradation rate in more detail. Kinetic analysis based on the L-H kinetics model was carried out from Eq. (1).

$$r_0 = \frac{kKC_0}{1 + KC_0} \text{ or } \frac{1}{r_0} = \frac{1}{k} \frac{1}{C_0} + \frac{1}{k} \quad (1)$$

where r_0 is initial photocatalytic degradation rate ($\mu\text{M} \times \text{h}^{-1}$), C_0 the initial reaction concentration of IPA (μM), k the reaction rate constant ($\mu\text{M} \times \text{h}^{-1}$) and K is the Langmuir adsorption constant (μM^{-1}).

A linear plot of $1/r_0$ versus $1/C_0$ was obtained with regression coefficient greater than 0.985 in this work. Fig. 7 shows plot of the reciprocal of the initial reaction rate versus the reciprocal of the five initial reaction levels of IPA. The kinetic parameters k and K were obtained from the intercept and slope of the straight line, respectively. Table 4 showed the dependence of treating time on reaction rate constant and adsorption constant. For TiO₂ samples treated for 30 and 60 min, the values of k and K were higher than those of plain TiO₂, especially for K . Some recent researches [21] confirmed that oxygen vacancies help in the trapping of photogenerated electrons, thus limiting the electron-hole recombination, which contributed to the enhance-

Table 4
Effect of treating time on reaction rate constant (k) and adsorption constant (K) of TiO₂ powders under visible light irradiation

Sample	k ($\mu\text{M} \times \text{h}^{-1}$)	K ($\mu\text{M} \times \text{h}^{-1}$)
ST-01	1.98	0.80
ST-01/30 min	2.80	1.71
ST-01/60 min	2.64	1.78

Table 5
Mineralization of plain and N₂-plasma heat-treated TiO₂ powders after 720 min of visible (VIS) or ultraviolet (UV) light irradiation

Sample	VIS-irradiation (%)	UV-irradiation (%)
ST-01	39.9	70.9
ST-01/10 min	78.7	–
ST-01/30 min	97.8	78.3
ST-01/60 min	80.8	76.7
ST-01/120 min	68.4	–

ment of photocatalytic activity. However, it must be taken into account that too much oxygen vacancies could act as recombination centers for electron–hole pairs [23], although the TiO₂ treated for 120 min exhibited the most oxygen vacancies but the lowest photoactivity. To determine the durability of treated sample in photocatalytic activity, the TiO₂ treated for 30 min stored at room temperature after 2 months was also examined by kinetic analysis. The value of *k* and *K* was 2.55 and 1.66, respectively. Fortunately, the result indicted that there was only a slight decrease as compared to the freshly treated TiO₂ powder.

In order to clarify the role of oxygen vacancies of treated TiO₂ in the photocatalytic reaction, the experiments of the mineralization yield of gaseous IPA under two different light sources (fluorescent light lamp and ultraviolet lamp) were conducted for three samples, such as the plain and treated for 30 and 60 min TiO₂. The mineralization yield of gaseous IPA is defined as follows [24]:

$$\text{mineralization (\%)} = \frac{1/3[\text{CO}_2]_{\text{production}}}{[\text{CH}_3\text{CHOHCH}_3]_{\text{original}}} \times 100\%$$

When 100% mineralization yield occurs, 3 mol of carbon dioxide are formed from each mole of IPA. The results of mineralization yield after 720 min of visible or ultraviolet light illumination were listed in Table 5. The plain ST-01 revealed high photocatalytic activity under UV irradiation, while it showed slightly considerable mineralization yield in visible light. In this study, ST-01 is still visible-light-active, since the illumination of white fluorescent light lamp is comprised of about 3–5% ultraviolet light. The TiO₂ samples treated for 30 and 60 min exhibited high activity in both UV and visible light, and the mineralization yield in visible light was discernible higher than that of in UV. These results confirm that these two treated TiO₂ were more visible-light-active compared to plain ST-01 under visible light illumination, due to the formation of oxygen vacancies induced by the thermal N₂-plasma surface treatment. As can be seen from Fig. 2, TiO₂ treated for 120 min showed the highest absorption in visible light region. However, this catalyst has lowest mineralization yield among the treated samples. Thus, it is concluded that enhanced absorption of visible light is a necessary condition but not a sufficient condition for the visible-light-active photocatalyst. As mentioned above, the TiO₂ treated for 30 min had the highest reaction rate constant as well as CO₂ formation. It can also be noticed that an intermediate level of visible-light absorption level combined with optimum structure defects (oxygen vacancies) render the TiO₂ treated for 30 min the highest photocatalytic activity.

4. Conclusions

The visible-light-photoactive TiO₂ powders were prepared by thermal N₂-plasma treatment at RF power of 400 W and the heating temperature of 400 °C for the different treating periods. The treating time greatly influenced the visible light absorption, BET surface, IPA adsorption and photocatalytic activity of the prepared TiO₂ samples. The XPS results showed that during the N₂-plasma surface treatment, the oxygen vacancies were produced and attributed to the increase of visible absorbance and the enhancement of photocatalytic activity. For powders treated for 30 min, the photocatalytic activity of TiO₂ exhibited the highest photoactivity with an intermediate level of visible-light absorption level as well as optimum oxygen vacancies. The thermal N₂-plasma method was proved to modify the surface of TiO₂ by means of the introduction of oxygen vacancies and the experimental results confirmed the enhanced photocatalytic activities of treated TiO₂ were not the contribution of doped nitrogen atoms but the oxygen vacancies.

Acknowledgement

The authors are grateful to the support by the National Science Council of Republic of China under grant NSC 91-2622-E-168-012-CC3.

References

- [1] T. López, R. Gómez, G. Pecci, P. Reyes, X. Bokhimi, O. Novaro, *Mater. Lett.* 40 (1999) 59–65.
- [2] J. Engweiler, J. Harf, A. Baiker, *J. Catal.* 159 (1996) 259–269.
- [3] V. Pore, M. Heikkilä, M. Ritala, M. Leskela, S. Areva, *J. Photochem. Photobiol. A: Chem.* 177 (2006) 68–75.
- [4] S.U.M. Khan, M. Al-Shahry, W.B. Ingler Jr., *Science* 297 (2002) 2243–2245.
- [5] T. Ohno, M. Akiyoshi, T. Umebayashi, K. Asai, T. Mitsui, M. Matsumura, *Appl. Catal. A: Gen.* 265 (2004) 115–121.
- [6] R. Asahi, T. Morikawa, T. Ohwaki, K. Aoki, Y. Taga, *Science* 293 (2001) 269–274.
- [7] M.C. Yang, T.S. Yang, M.S. Wong, *Thin Solid Films* 469–470 (2004) 1–5.
- [8] S. Sato, R. Nakamura, S. Abe, *Appl. Catal. A: Gen.* 284 (2005) 131–137.
- [9] D. Li, H. Haneda, S. Hishita, N. Ohashi, *Mater. Sci. Eng. B: Solid* 117 (2005) 67–75.
- [10] T. Ihara, M. Miyoshi, Y. Iriyama, O. Matsumoto, S. Sugihara, *Appl. Catal. B: Environ.* 42 (2003) 403–409.
- [11] H. Irie, Y. Watanabe, K. Hashimoto, *J. Phys. Chem. B* 107 (2003) 5483–5486.
- [12] T. Ihara, M. Miyoshi, M. Ando, S. Sugihara, Y. Iriyama, *J. Mater. Sci.* 36 (2001) 4201–4207.
- [13] W.Z. Tang, H. An, *Chemosphere* 31 (1995) 4157–4170.
- [14] A.M. Peiró, J.A. Ayllón, J. Peral, X. Doménech, *Appl. Catal. B: Environ.* 30 (2001) 359–373.
- [15] A. Bouzaza, A. Laplancheb, *J. Photochem. Photobiol. A: Chem.* 150 (2002) 207–212.
- [16] S.B. Kim, S.C. Hong, *Appl. Catal. B: Environ.* 35 (2002) 305–315.
- [17] E. McCafferty, J.P. Wightman, *Surf. Interface Anal.* 26 (1998) 549–564.
- [18] Y. Sakatani, J. Nunoshige, H. Ando, *Chem. Lett.* 32 (2003) 1156–1157.
- [19] J.L. Gole, J.D. Stout, C. Burda, Y. Lou, X. Chen, *J. Phys. Chem. B* 108 (2004) 1230–1240.
- [20] K. Takeuchi, I. Nakamura, O. Matsumoto, S. Sugihara, M. Ando, T. Ihara, *Chem. Lett.* (2000) 1354–1355.

- 400 [21] I. Nakamura, N. Negishi, S. Ktusuna, T. Ihara, S. Sugihara, K. Takeuchi, 404
401 J. Mol. Catal A: Chem. 161 (2000) 205-212. 405
402 [22] T. Ishigaki, H. Haneda, N. Okada, S. Ito, Thin Solid Films 390 (2001) 406
403 20-25. 407
- [23] H. Irie, Y. Watanabe, K. Hashimoto, J. Phys. Chem. B 107 (2003) 404
5483-5486. 405
- [24] X. Fu, W.A. Zeltner, M.A. Anderson, Appl. Catal. B: Environ. 6 (1995) 406
209-224. 407

UNCORRECTED PROOF